Abrupt Transition to Strong Superrotation in an Axisymmetric Model of the Upper Troposphere

KAREN M. SHELL

Scripps Institution of Oceanography, University of California, San Diego, La Jolla, California

ISAAC M. HELD

NOAA/Geophysical Fluid Dynamics Laboratory, Princeton, New Jersey

ABSTRACT

Abrupt transitions to strongly superrotating states have been found in some idealized models of the troposphere. These transitions are thought to be caused by feedbacks between the eddy momentum flux convergence in low latitudes and the strength of the equatorial flow. The behavior of an axisymmetric shallow-water model with an applied tropical torque is studied here to determine if an abrupt transition can be realized without eddy feedbacks. The upper-tropospheric layer is relaxed to a radiative equilibrium thickness, exchanging mass and thus momentum with the nonmoving lower layer. For low values of the applied torque, the circulation is earthlike; however, for larger values, an abrupt transition to a strongly superrotating state can occur. In some cases, the system remains superrotating as the torque is subsequently decreased. A simple analytical model is used to better understand the system. The bifurcation is caused by a feedback between the applied torque and the strength of the Hadley cell. As the torque increases, the strength of the cell decreases, reducing the damping caused by momentum transfer from the lower layer.

1. Introduction

Given the zonal mean zonal flow u, one can compute the corresponding absolute angular momentum about the axis of rotation

$$M \equiv a \cos\phi(\Omega a \cos\phi + u), \qquad (1)$$

where a is the radius of the planet, Ω the rotation rate, and ϕ the latitude. We use the term *superrotating* to refer to an atmosphere in which M at some latitude or height exceeds Ωa^2, the angular momentum of the surface of the planet at the equator. Since the maximum angular momentum of the solid planet is found at the equator, a superrotating atmosphere achieves a value of M larger than any surface values. In order for the circulation to be inertially stable, M must decrease poleward; thus equatorial winds invariably have the greatest angular momentum. Therefore, on a counterclockwise rotating planet, an atmosphere is superrotating if and only if the winds at the equator are westerly.

Maintenance of superrotation requires the transport of angular momentum from areas of low angular momentum to the region of maximum angular momentum at the equator. Assuming that such countergradient fluxes exist, the strength of the superrotation is then determined by the response of the processes that decelerate the equatorial winds (e.g., poleward momentum fluxes or advection from regions of smaller M) to the equatorial acceleration.

On the earth, the mean equatorial tropospheric winds are slightly easterly. Thus, the earth's troposphere is not superrotating. However, superrotation occurs during the westerly phase of the quasi-biennial oscillation (QBO) in the stratosphere, as well as on other planets, such as Jupiter and Saturn, and on our sun. These cases raise the question of whether the earth's troposphere could be superrotating under somewhat different conditions.

Strong superrotation has in fact been simulated in some simple models of the earth's atmosphere. Suarez and Duffy (1992) obtain superrotating states in a two-layer model when they apply a zonally asymmetric tropical heating. For certain strengths of the heating, they find multiple equilibria. Once superrotation is established in the model, the system remains superrotating, even if they remove the asymmetric heating. Saravanan (1990) uses a two-layer model as well but applies a zonally symmetric torque, rather than asymmetric heating, to produce superrotation, so as to study the feedbacks between eddy fluxes and equatorial winds in the simpler setting of a model with a zonally symmetric

Corresponding author address: Karen M. Shell, University of California, San Diego, 9500 Gilman Dr., Dept. 0224, La Jolla, CA 92093-0224.
E-mail: kshell@ucsd.edu

climate. Suarez and Duffy (1992) and Saravanan (1990) attribute the abrupt transitions to strong superrotation to a feedback between the equatorial acceleration (whether generated by asymmetric heating or an applied torque) and the deceleration due to poleward eddy angular momentum flux in the Tropics. Strong winds make the Tropics more transparent to Rossby waves, decreasing the strength of the eddy deceleration. This weakened deceleration, in turn, results in stronger equatorial winds and a positive feedback.

Williams (2003) obtains superrotation in a dry multilayer primitive equation model by moving the location of maximum baroclinicity equatorward. Williams describes a different process than Suarez and Duffy (1992) and Saravanan (1990), attributing the acceleration to an equatorward eddy flux generated by barotropic instability when the jet is close to the equator, but feedbacks with the background poleward momentum fluxes still play a central role, resulting in abrupt transitions between a superrotating and nonsuperrotating state.

Using an axisymmetric (no variation in the longitudinal direction) model, we examine a different feedback in a superrotating atmosphere, one that can occur in the absence of wave–mean flow interactions. In order to obtain equatorial westerlies, we specify a torque in the Tropics. These superrotating equatorial winds are decelerated by the Hadley circulation, which advects a smaller M from below. The strength of the deceleration caused by the Hadley circulation depends on tropical temperature gradients and, therefore, on the wind speed at the equator. We are interested in whether this feedback allows multiple equilibria for some ranges of the imposed forcing. Since the equatorial zonal wind is always westerly when forcing is applied to this model, we look for multiple steady superrotating states, one weakly superrotating and one strongly superrotating, for the same set of parameters.

In order to illustrate the mechanism in the simplest context, we use a shallow-water model of the upper troposphere. We also provide a generalization of the Held–Hou Hadley cell theory to allow for nonzero equatorial winds and use this analytical model to explain the shallow water results. By focusing on this axisymmetric feedback mechanism, we do not mean to imply that the eddy feedbacks discussed elsewhere are neither important nor dominant. However, we think it is useful to keep in mind this axisymmetric mechanism as well.

2. The model

We model the troposphere using an axisymmetric 1½-layer model. The lower layer does not move, but it can affect the thickness and zonal velocity of the upper layer through the exchange of mass. The upper layer is modeled using the shallow-water equations for a spherical isentropic layer. The model determines the zonal velocity u, meridional velocity v, and thickness of the upper layer h as a function of time t, and latitude ϕ:

$$\frac{\partial u}{\partial t} + \frac{v}{a}\frac{\partial u}{\partial \phi} - 2\Omega v \sin\phi - \frac{uv\tan\phi}{a} = F + R - ku \quad (2)$$

$$\frac{\partial v}{\partial t} + \frac{v}{a}\frac{\partial v}{\partial \phi} + 2\Omega u \sin\phi + \frac{u^2\tan\phi}{a} = -\frac{g^*}{a}\frac{\partial h}{\partial \phi} - kv \quad (3)$$

$$\frac{\partial h}{\partial t} + \frac{1}{a\cos\phi}\frac{\partial hv\cos\phi}{\partial \phi} = -\frac{h - h_{eq}}{\tau}, \quad (4)$$

where Ω is the rotation rate, a is the radius of the earth, k is the frictional parameter, and g^* is the reduced gravity; F is an applied forcing, and the system is relaxed to a radiative equilibrium thickness $h_{eq}(\phi)$ with relaxation time τ and resulting effect on zonal momentum, R.

The relaxation of the layer thickness to the "radiative equilibrium" thickness h_{eq} simulates the effect of radiation on the system. The radiative equilibrium thickness decreases away from the equator and then approaches a constant poleward of latitude ϕ_h:

$$h_{eq} = \begin{cases} h_{0eq} - \dfrac{a\Omega}{g^*}u_{0eq}\sin^2\phi & (|\phi| < \phi_h) \\[2ex] h_{0eq} - \dfrac{a\Omega}{g^*}u_{0eq}\sin^2\phi_h & (|\phi| \geq \phi_h), \end{cases} \quad (5)$$

where h_{0eq} is the radiative equilibrium thickness at the equator and u_{0eq} is the corresponding equatorial wind. This relaxation creates a Hadley circulation. In the Tropics, the layer thickness is generally smaller than the radiative equilibrium thickness; thus, the relaxation term increases the layer thickness, corresponding to a mass flux from below (i.e., the upward branch of the Hadley cell). In the subtropics, the layer thickness is generally higher than the radiative equilibrium thickness, and the relaxation term models the downward branch of the cell. We are interested in the interaction between the Hadley cell and the tropical zonal wind and, since the high-latitude profile of h_{eq} makes little difference to the results presented here, we simplify the problem by restricting the winds to the Tropics and subtropics. (If we were to use the $\sin^2$ profile at all latitudes, the layer thickness would become too small at the poles.)

The forcing F for the system is an applied torque centered around the equator, constant in time:

$$F = F_0 \cos^n\phi, \quad (6)$$

where F_0 is the forcing at the equator, and n is used to vary the shape of the forcing. We apply a torque in order to generate westerlies at the equator and study feedbacks between the wind speed and the axisymmetric Hadley circulation. The forcing mechanism is unspecified and unimportant for our purposes since it is assumed not to respond to the state of the upper layer. One can think of it as due to a longitudinally asymmetric process, such as organized tropical convection, which produces a low-latitude eddy momentum flux convergence. We have also generated solutions in which ac-
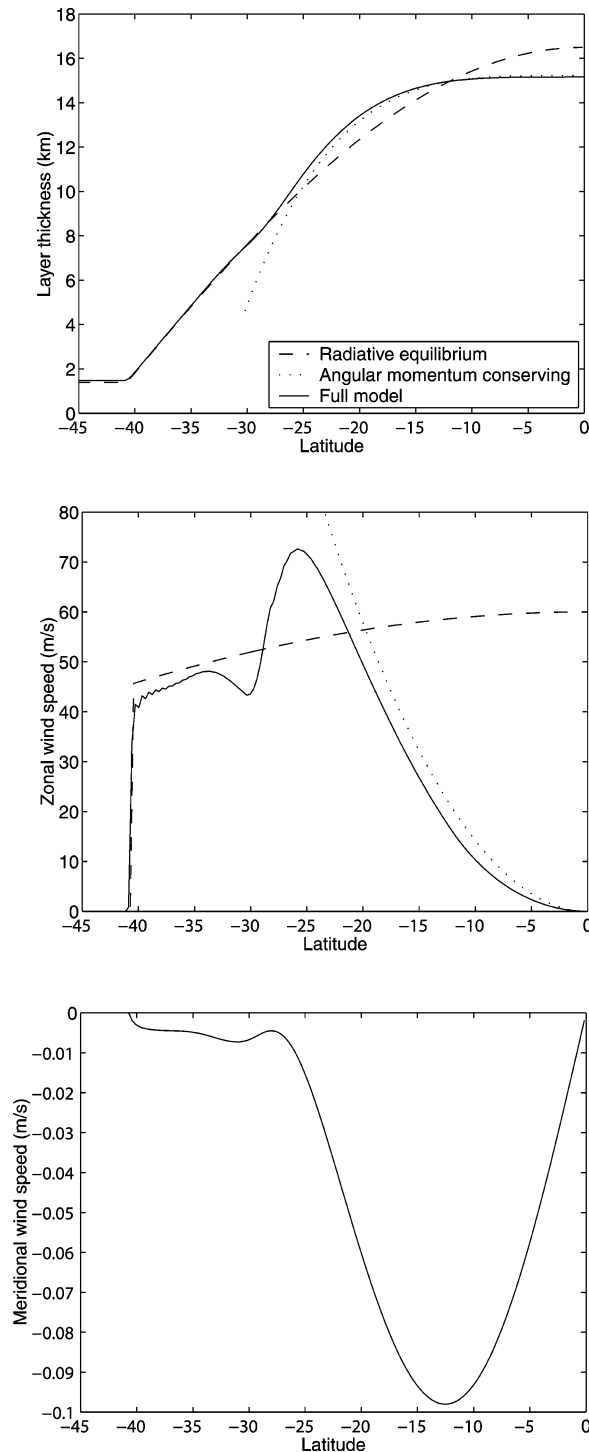
FIG. 1. Steady state of the model with no forcing. The solid lines are the computational model results. The dotted lines indicate thickness and zonal winds from momentum conservation, and the dashed lines are the radiative equilibrium profiles. High-latitude results are omitted in this and all future figures since the zonal and meridional winds are zero and the thickness is constant.

celeration in the Tropics is balanced by deceleration in midlatitudes. The results are essentially unchanged; the key quantity is the equatorial acceleration.

The term R represents the effect of mass exchange with the lower layer on the momentum of the upper active layer. Setting $Q \equiv (h_{eq} - h)/\tau$,

$$R = \begin{cases} -Qu/h, & (Q > 0) \\ 0, & (Q < 0). \end{cases} \tag{7}$$

Air that is brought up from the lower layer carries with it the zero relative angular momentum of that layer. Since there is normally rising motion at the equator, this term provides damping of the westerly equatorial flow. Air that moves from the upper layer down to the lower layer carries with it the momentum of the upper layer and thus does not affect the upper-layer momentum. One can think of surface friction as rapidly returning the velocity in the lower layer to zero. Here R is equivalent to the vertical advection of zonal momentum in multilevel models. [Note that the momentum transport associated with the mass flux should also affect the meridional velocity. However, we have omitted this effect from Eq. (3) because the model is always very close to geostrophic balance.]

The deceleration of zonal wind by the upward advection of zero angular momentum air in the rising branch of the Hadley cell is central to the model because it provides the potential for positive feedback as the applied forcing F is increased. At the equator, the applied force must be balanced by the combination of momentum exchange, R, and frictional drag, $-ku$. We expect an abrupt transition to strong superrotation if the combined deceleration provided by the momentum exchange and friction fails at some point to offset the applied forcing. Since stronger forcing leads to higher zonal wind speeds and thus stronger frictional drag, the upward mass flux at the equator Q must decrease sharply as the applied force F increases in order for a runaway positive feedback to occur.

The model is solved numerically using a centered in space, leapfrog in time scheme with a Robert (asselin) filter to prevent time splitting. The grid is staggered, with u and h grid points halfway between the v grid points. The poles correspond to v grid points, and v is set to 0 there. The equator is a u and h grid point. Rather than solve the u equation directly, we actually solve the absolute angular momentum equation so that the advection of angular momentum accounts for the Coriolis and metric terms. We then set

$$\frac{\partial u}{\partial t} = \frac{1}{a \cos\phi} \frac{\partial M}{\partial t}$$

to determine the corresponding u tendency.

We search for stable equilibrium solutions of the model by integrating Eqs. (2) through (4) until we reach a steady state. The solid lines in Fig. 1 show the steady state of the model with no forcing. We use values of

$a = 6.37 \times 10^6$ m, $\Omega = 7.292 \times 10^{-5}$ rad s^{-1}, $g^* = 0.08g$ with $g = 9.81$ m s^{-2}, $\tau = 8 \times 10^5$ s, $k = 10^{-8}$ s^{-1}, $h_{0eq} = 16\,500$ m, $u_{0eq} = 60$ m s^{-1}, and $\phi_h = 40.5°$. Later, when forcing is applied, we use a forcing shape factor $n = 30$ [see Eq. (6)], which results in a half width for the forcing of roughly 12° latitude. These are the default values for all runs.

It is difficult to make this shallow-water model fully earthlike. Because the observed isentropic slope roughly carries an isentropic interface from the surface in the Tropics to the tropopause at the pole, our layer thickness is inevitably large at the equator. As a consequence, the friction must be very weak to avoid diffusive domination. To mimic the effects of a small gross moist stability (Neelin and Held 1987) and the associated strong meridional flow, one would require just the opposite, a very thin layer in the Tropics. If one tries to make the layer thinner to strengthen the flow, one encounters problems with large Froude numbers due to the fact that the transition to no flow in the lower layer is occurring too rapidly in the vertical. More layers and some representation of moist stability or latent heat transport are needed to create a more realistic model. However, we believe that the feedback captured in this simple dry model will be present in more realistic models of the Hadley cell if these models are sufficiently inviscid.

3. Analytical calculations

Before presenting solutions with nonzero F, we approximate the full system of equations with a simple analytical model in order to gain insight into the possibility for bifurcation. The model relates the zonal wind and layer thickness at the equator. We then determine which zonal wind values result in steady states for a given set of parameters. These equilibrium solutions suggest parameter ranges where multiple equilibria are expected in the full model.

The relation of equatorial zonal wind u_0 to equatorial layer thickness h_0 can be explored using a simple Hadley cell model similar to the one used in Held and Hou (1980). The domain is divided into two regions. Close to the equator, the thickness h_m is in geostrophic balance with the angular momentum conserving wind:

$$u_m = \frac{u_0 + \Omega a \sin^2\phi}{\cos\phi}. \tag{8}$$

Integrating the geostrophic terms in Eq. (3) using the small angle approximation and the fact that $u_0 \ll \Omega a$,

$$h_m = h_0 - \frac{2a\Omega}{g^*}\left[u_0\frac{\phi^2}{2} + \Omega a\frac{\phi^4}{4}\right]. \tag{9}$$

Toward the poles, the thickness is just the radiative equilibrium solution, h_{eq} [Eq. (5)]. The thickness transitions from one solution to the other at the critical latitude ϕ_c, where it is continuous:

$$h_{eq}(\phi_c) = h_m(\phi_c). \tag{10}$$

In addition, mass conservation requires

$$\int_0^{\phi_c} h_{eq} \cos\phi \, d\phi = \int_0^{\phi_c} h_m \cos\phi \, d\phi. \tag{11}$$

Assuming $u_0 \ll \Omega a$, $h_{0eq} \approx h_0$, and $\phi_c \ll 1$, we obtain equations for the critical latitude and the thickness at the equator in terms of u_0:

$$\phi_c^2 = \frac{5}{3}\frac{u_{0eq} - u_0}{\Omega a}$$

$$h_0 - h_{0eq} = -\frac{5}{18g^*}(u_{0eq} - u_0)^2. \tag{12}$$

Note that to get a real value for ϕ_c, u_0 must be less than u_{0eq}.

Figure 1 compares the full model to the simple Hadley cell model for the case of no forcing (corresponding to $u_0 = 0$). Near the equator, the full model thickness closely follows the angular momentum conserving solution; it transitions to the radiative equilibrium solution slightly poleward of the critical latitude. The full model does not exactly match the simple analytical model because it does not completely conserve angular momentum, due to friction and the flux of momentum from the lower layer. Nevertheless, the simple Hadley cell model seems a reasonable approximation to the full system of equations.

To obtain a steady state in the presence of forcing, the applied torque at the equator must balance deceleration caused by friction and momentum exchange with the lower layer:

$$F = \frac{h_{0eq} - h_0}{\tau}\frac{u_0}{h_0} + ku_0 \qquad (h_0 < h_{0eq}). \tag{13}$$

The key assumption here is that we need to consider only the equatorial effects of the drag due to momentum exchange with the lower layer. Away from the equator, we continue to assume that angular momentum conservation is an adequate approximation.

Assuming the system is not far from radiative equilibrium, we approximate the thickness in the denominator as a constant h_{0eq}. (Retaining the variation of thickness in the denominator does not greatly alter the solution.) Nondimensionalizing by

$$h_0 = Hh_{0eq}, \qquad u_0 = Uu_{0eq},$$

Eqs. (12) and (13) become

$$1 - H = p(U - 1)^2 \tag{14}$$

$$1 - H = \frac{q}{U} - r, \tag{15}$$

where

$$p = \frac{5}{18}\frac{u_{0eq}^2}{g^*h_{0eq}}, \qquad q = \frac{F\tau}{u_{0eq}}, \qquad r = k\tau.$$
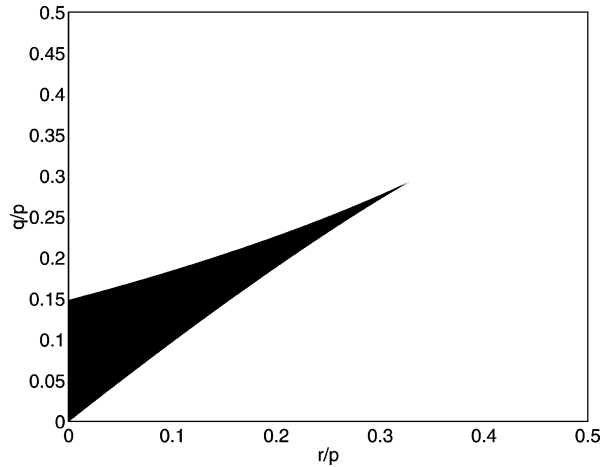
FIG. 2. Region of multiple equilibria in the analytical model. The dark region indicates values of r/p and q/p for which there exist multiple equilibria; q corresponds to the strength of the applied forcing, r corresponds to the friction, p relates to the Hadley circulation.

FIG. 3. Equatorial angular momentum terms as a function of u_0.

All three parameters are positive; q is proportional to the imposed forcing, r to the frictional damping, and p to the square of the Froude number at the equator in the unforced radiative equilibrium solution.

Combining Eqs. (14) and (15) to obtain a cubic equation,

$$U^3 - 2U^2 + U\left(1 + \frac{r}{p}\right) - \frac{q}{p} = 0. \qquad (16)$$

The system is governed by two nondimensional parameters, r/p and q/p. The equation has three real solutions when

$$\left(-\frac{1}{9} + \frac{1}{3}\frac{r}{p}\right)^3 + \left(-\frac{1}{27} - \frac{1}{3}\frac{r}{p} + \frac{1}{2}\frac{q}{p}\right)^2 < 0. \qquad (17)$$

Otherwise, there is only one real solution, and we do not expect multiple equilibria in our model. Note that valid solutions are within the range $U < 1$ and $0 < H < 1$ since our analytical model requires that $u_0 < u_{0eq}$ and $0 < h_0 < h_{0eq}$.

Figure 2 shows the parameter region where the simple model predicts multiple equilibria. There are three solutions in this region. If one adds time dependence to this analytical model by including the time derivative of the angular momentum at the equator in the equatorial momentum budget, one finds that the solution corresponding to the smallest u_0 is stable while the middle solution is unstable. [The stability of the solutions of the analytical model can be verified using a potential function (J. Moehlis 2000, personal communication)]. Model runs that start with initial conditions between the lowest and the middle solutions will equilibrate to the lowest superrotating state.

The third solution (highest u_0) is also stable; thus we expect the system to go to this state if the initial con-
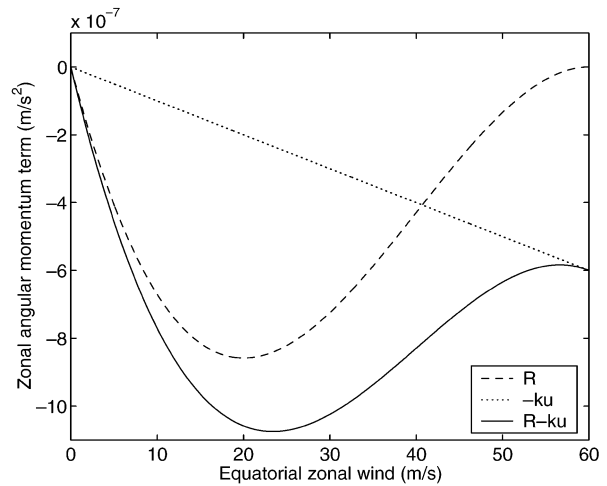
ditions are above the middle solution. However, the solution with the highest u_0 obtained with our analytical model is often not valid because $u > u_{0eq}$, and therefore, the Hadley cell model [Eq. (12)] is no longer valid. The full system (described in the next section) still equilibrates, but we do not offer a simple quantitative model of the final equilibrated strongly superrotating state.

In order to understand the transition to the strongly superrotating state, we further examine the relationship between the zonal wind and the deceleration by the upward branch of the Hadley cell. As the forcing increases, u_0 increases, which in turn decreases the Hadley circulation. The resulting deceleration of the zonal wind by the Hadley cell depends on the vertical mass flux, which decreases as the zonal wind increases, and the vertical wind shear, which increases as the zonal wind increases. To determine the net effect of the zonal wind on R, we use Eq. (12) to solve for R [Eq. (7)] in terms of u_0:

$$R = \frac{u_0}{\tau}\left[\frac{-5(u_{0eq} - u_0)^2}{18g^*h_{0eq}}\right]. \qquad (18)$$

The dashed line in Fig. 3 shows the response of R to u_0. When u_0 is small, R decreases as u increases, R reaches its minimum value when $u_0 = u_{0eq}/3$ ($U = 1/3$). When U is greater than this value, R becomes less negative. Thus, in the frictionless case, we expect the deceleration caused by the upward branch of the Hadley cell to no longer be able to balance increases in applied forcing when $U = 1/3$.

When both friction and the vertical advection of momentum are included (solid line in Fig. 3), the maximum and minimum decelerations are found at

$$U = \frac{2 \pm \sqrt{1 - (3r/p)}}{3}.$$

The minus sign corresponds to the maximum weakly superrotating U, where the deceleration terms begin de-

creasing in magnitude with increasing U, while the upper value (assuming it is valid) corresponds to the minimum strongly superrotating U, where the deceleration terms begin increasing in magnitude with decreasing U. When $r/p > 1/3$, U never jumps to a different branch as the flow is too frictionally dominated.

Using the variable values listed in section 2, the nondimensional parameters are $p = 0.0772$, $r = 0.008$, and $q = 13\,333 \times F_0$. The asterisks and $\times$s in Fig. 4 show the steady states in the simple model. The asterisks correspond to stable solutions, while the $\times$s indicate unstable solutions. The maximum U on the lower branch is 0.39, corresponding to an applied forcing of 10.1×10^{-7} m s^{-2}. The minimum U on the upper branch is 0.94 ($F_0 = 5.8 \times 10^{-7}$ m s^{-2}). For this set of parameters, there are valid upper branch solutions (i.e., where $U < 1$) for a small range of applied forcing. However, most of the upper branch solutions are invalid.

Thus, the simple model predicts an abrupt transition from weak to strong superrotation. However, the model does not always predict valid strongly superrotating states since Held–Hou theory no longer applies. Furthermore, the simple model unrealistically assumes that the applied forcing affects the angular momentum budget only at the equator. Finally, the statements concerning the stability of the different equilibria in the analytical model ignore the time dependence associated with the adjustment of the Hadley cell to these equatorial conditions. To address these limitations, we explore the behavior of an axisymmetric atmosphere using a computational model.

4. Results from the full model

We next look for multiple equilibria in the full model by integrating our shallow-water system to steady states using different initial conditions and forcing magnitudes. We sampled the forcing in increments of 2×10^{-8} m s^{-2}. There are two distinct branches of solutions, one similar to the simple angular momentum conserving Hadley cell model (weakly superrotating) and one strongly superrotating. The open circles in Fig. 4 show how U changes with the forcing. As the forcing increases from zero, the zonal wind increases, abruptly transitioning to strong superrotation at $F_0 = 9.2 \times 10^{-7}$ m s^{-2}. When the forcing is subsequently decreased, the model remains strongly superrotating until the forcing is reduced to 7.6×10^{-7} m s^{-2}. The results can be classified into four regions of different behavior depending on the magnitude of the forcing at the equator, F_0.

1) For small forcing, there is only one stable solution, with a small zonal velocity at the equator. The zonal wind and layer thickness approximately agree with the simple analytical Hadley cell model; near the equator, angular momentum is approximately conserved. At the equator, the thickness relaxation term
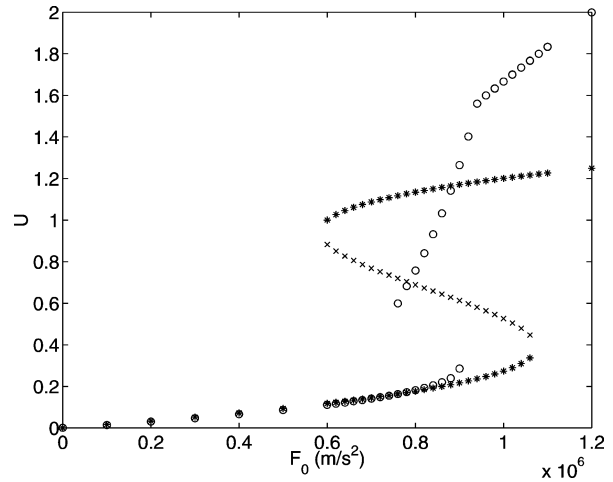

FIG. 4. Nondimensional zonal wind at the equator for a range of equatorial forcing values. Circles correspond to full model results, asterisks to stable solutions of the analytic model, and $\times$'s to unstable solutions. Analytic solutions with $U > 1$ are not valid and are shown for illustrative purposes only.

[Eq. (7)] in the zonal momentum equation [Eq. (2)] increases with increasing F, and friction is weak. The dashed lines in Fig. 5 show a sample steady solution in this region.

2) For somewhat higher forcing, the system has two steady solutions. The lower branch approximates the Hadley cell model, while the upper branch has a very weak Hadley circulation. The upper solution layer thickness is close to the equilibrium thickness; the zonal momentum is far from angular momentum conservation; and the meridional wind is small. In the lower branch, similar to region 1, equatorial relaxation toward radiative equilibrium always increases in magnitude and dominates friction, while in the upper branch, the magnitude of R decreases so that it is similar to the frictional term. The dashed–dotted lines in Fig. 5 show a sample steady lower branch solution, while the dotted lines show a steady upper branch solution in this region.

3) When the forcing is further increased, the system has only one steady state, similar to the upper solution of region 2. As the forcing increases, an equatorial jet develops and strengthens. Generally u is above u_{0eq}, but h is always below h_{eq}. The Hadley cell is weak but still present. The relaxation term always decreases with increasing F, so the friction term dominates by the high end of the region. The thin solid lines in Fig. 5 show a sample steady solution in this region.

4) For the highest values of the forcing, h_0 is above h_{0eq}. This corresponds to a collapse of the Hadley circulation, with sinking at the equator and rising slightly poleward of the equator. Thus the only zonal momentum tendency term that can balance the forc-
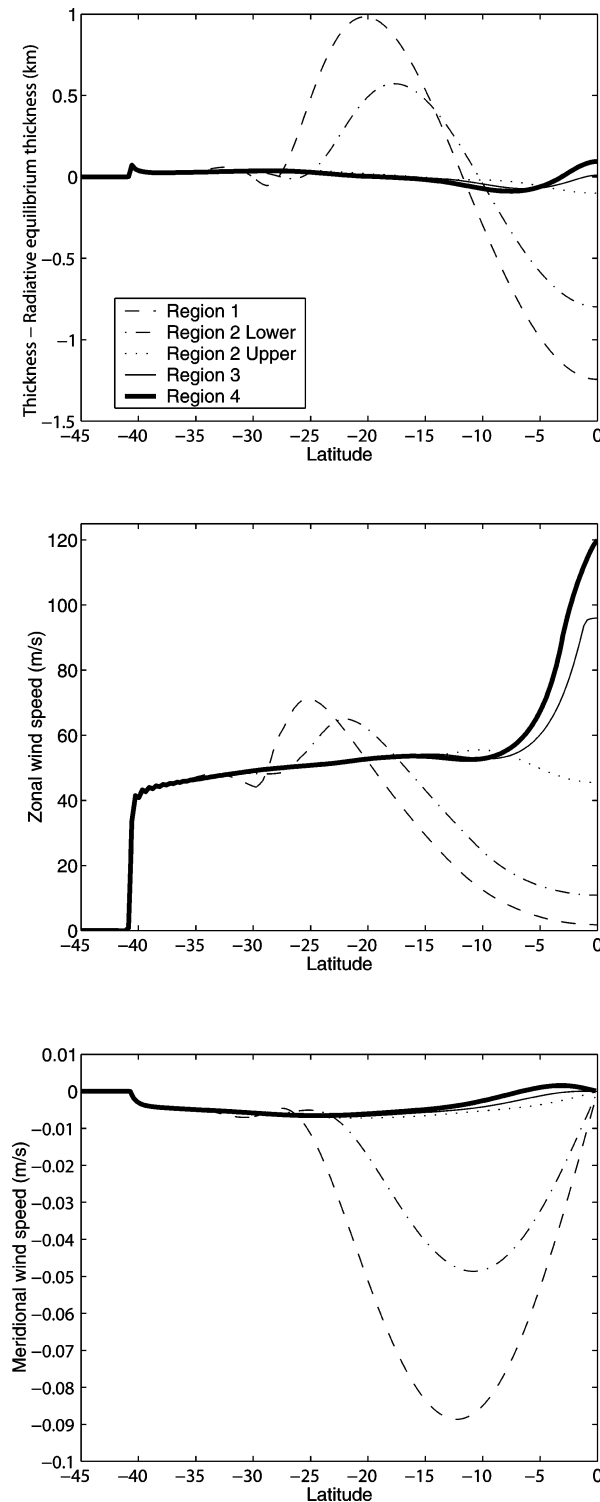
FIG. 5. Model steady states for $F_0 = 2 \times 10^{-7}$ m s^{-2} (dashed), 8 $\times 10^{-7}$ m s^{-2} lower branch (dashed–dotted), 8 $\times 10^{-7}$ m s^{-2} upper branch (dotted), 9.6 $\times 10^{-7}$ m s^{-2} (thin), and 12 $\times 10^{-7}$ m s^{-2} (thick).

ing is friction, and u_0 has only one possible value:

$$u_0 = F_0/k.$$

Near the equator, the meridional winds reverse direction, flowing toward the equator rather than away. The equatorial jet is very strong. The thick solid lines in Fig. 5 show a sample steady solution in this region.

The location of the multiple steady equilibria region in the shallow-water model is thus within the predicted range [5.8 to 10.1 ($\times 10^{-7}$ m s^{-2})]. However, the range is less than that predicted by the simple model. For low values of the forcing F, the full model closely follows the predictions of the simple model. As the full model approaches the end of the lower branch, the solutions diverge since the simple model does not include any off-equatorial forcing. The maximum U on the lower branch is 0.29, smaller than the predicted value (0.39). The upper branch solutions are very different, including the minimum U (0.60), which is significantly lower than the predicted upper branch minimum of 0.94. The full model can no longer be well approximated by Held–Hou theory since angular momentum is no longer conserved (see the dotted and solid lines in Fig. 5). In addition, the simple model predictions are not valid for most of the upper branch solutions since $U > 1$. Thus, it is not surprising that the two models produce different results for the upper branch.

Although the simple model assumes that all momentum exchange occurs at the equator and thus does not depend on the shape of the forcing (the exponent n in particular), this shape does affect the full model's behavior to some extent by influencing the closeness of the model to angular momentum conservation. As a result, similar runs (not shown) with different values of n have different ranges of multiple equilibria. However, the runs display qualitatively similar behavior.

Finally, we explore the system behavior as we vary the frictional parameter k. As k increases, the region of multiple equilibria contracts and moves to higher values of the forcing F until the system becomes too frictionally damped and no abrupt transition occurs, as predicted by the simple model. The transition to the single solution region occurs for a smaller k than predicted by the simple model, consistent with the smaller range of multiple equilibria found in the F experiments of the full model.

5. Conclusions

It is possible to get bifurcations in the superrotation strength of an axisymmetric model for earthlike parameter ranges. When bifurcations exist, the stable equilibria lie along two branches of zonal wind values as the forcing is changed. On the lower branch, damping due to vertical advection of momentum by the Hadley cell increases with increasing forcing; on the upper branch, the damping decreases with increasing forcing. Al-

though the simple model approximately predicts where the full model will have multiple equilibria, the range is smaller than predicted and depends on the shape of the applied forcing. The presence and location of the bifurcation is related to how well angular momentum is conserved in the Tropics.

In our model, we directly apply a constant zonal acceleration centered around the equator. This forcing term represents the net effect of all the processes not explicitly included in the model, such as stationary and transient eddies as well as transient changes in the mean meridional circulation. Observed values of equatorial momentum flux convergence for these processes range from about -10×10^{-6} m s^{-2} for the transient meridional circulation to $+5 \times 10^{-6}$ m s^{-2} for stationary eddies (Lee 1999). Our model experiences an abrupt transition to superrotation when the net imposed acceleration is equal to 7.6×10^{-7} m s^{-2}, an order of magnitude less than the individual terms. However, the vertical mass flux in the unforced model is very small compared with the observed Hadley cell transport, as discussed in section 2. Assuming the ratio of the mass flux in the unforced model to the observed mass flux is approximately the ratio of the model's critical forcing to the actual critical forcing for the atmosphere, the critical forcing for an abrupt transition is much larger for the real atmosphere.

In a zonally asymmetric atmosphere, other feedbacks, such as the feedback between zonal winds and deceleration due to eddy flux divergence, which are not included in our model, may play the dominant role in an abrupt transition to superrotation. However, the feedback described here, between the wind speed and upward advection of momentum by the Hadley circulation, is capable of producing an abrupt transition in the absence of wave–mean flow interaction and may amplify transitions to superrotation in a zonally asymmetric atmosphere.

While abrupt transitions to superrotation are found in simplified models, they have not yet been found in comprehensive GCMs. Weak superrotation, on the other hand, has been observed. For example, Huang et al. (2001) found slight superrotation in a coupled GCM climate change simulation with tripled CO_2. More work is necessary to determine if an abrupt transition to strong superrotation is possible in the terrestrial setting.

REFERENCES

Held, I. M., and A. Y. Hou, 1980: Nonlinear axially symmetric circulations in a nearly inviscid atmosphere. *J. Atmos. Sci.,* **37,** 515–533.

Huang, H.-P., K. M. Weickmann, and C. J. Hsu, 2001: Trend in atmospheric angular momentum in a transient climate change simulation with greenhouse gas and aerosol forcing. *J. Climate,* **14,** 1525–1534.

Lee, S., 1999: Why are the climatological zonal winds easterly in the equatorial upper troposphere? *J. Atmos. Sci.,* **56,** 1353–1363.

Neelin, J. D., and I. M. Held, 1987: Modeling tropical convergence based on the moist static energy budget. *Mon. Wea. Rev.,* **115,** 3–12.

Saravanan, R., 1990: Mechanisms of equatorial superrotation: Studies with two-level models. Ph.D. thesis, Princeton University, 183 pp.

Suarez, M. J., and D. G. Duffy, 1992: Terrestrial superrotation: A bifurcation of the general circulation. *J. Atmos. Sci.,* **49,** 1541–1554.

Williams, G. P., 2003: Barotropic instability and equatorial superrotation. *J. Atmos. Sci.,* **60,** 2136–2152.